by nanopure water before melting at 4°C in a sterile HDPE container. Five-milliliter portions were placed in sterile test tubes and inoculated with isotopes to the following activities and concentrations: ^{14}C-bicarbonate (9.5×10^5 dpm ml^{-1}, trace addition), tritiated thymidine (2.1×10^8 dpm ml^{-1}; 36 nM), tritiated D-mannitol (2.2×10^8 dpm ml^{-1}; 7.5 nM), and tritiated L-amino acid mix (1.3×10^4 dpm ml^{-1}, 0.31 µg ml^{-1}). Three live replicates and one 5% formalin kill were included for each substrate addition. Samples were incubated in the dark at 4°C for 52 hours in air at 1 atm. Carbon 14–labeled bicarbonate and ^3H-labeled thymidine incubations were terminated by the addition of 0.5 ml of 6 M HCl and 5 ml of cold 10% trichloroacetic acid (TCA), respectively, before filtration onto 0.2-µm polycarbonate filters; ^3H-labeled mannitol incubations were terminated by filtration alone.

26. National Science Foundation Workshop–The Lake

Vostok Study: A Curiosity or a Focus for Interdisciplinary Investigations, Washington, DC, 7 to 8 September 1998 (see www.ldeo.columbia.edu/vostok/).
27. Ice for cultures was rinsed with −20°C ethanol, followed by autoclaved, distilled, and organic free water. The ice was melted at 4°C for 12 hours in an autoclaved HDPE bottle that had been rinsed with organic free, deionized water. One milliliter of melted core water was inoculated into two liquid media: phosphate (1.44 g liter^{-1} Na$_2$HPO$_4$ and 0.24 g liter^{-1} KH$_2$PO$_4$)-buffered sterile deionized water (pH 7.4) and sterile water containing 0.05% (w/v) peptone (pH 7.4). Meltwater (0.5 ml) was also spread onto sterile agar (15 g liter^{-1}) plates prepared with the same media. The inoculated media were incubated for 4 months at 4°C in air at 1 atm in the dark (liquid media preparations were on a shaker during incubation).
28. M. H. Carr et al., Nature 391, 363 (1998).

29. R. T. Pappalardo et al., J. Geophys. Res. 104, 24015 (1999).
30. R. Greenberg et al., Icarus 141, 263 (1999).
31. C. D. Takacs and J. C. Priscu, Microb. Ecol. 36, 239 (1998).
32. M. Legrand and P. Mayewski, Rev. Geophys. 35, 219 (1997).
33. Discussions with D. Karl, J. R. Petit, P. Price, J. Palais, B. Vaughn, and M. Edens helped improve the manuscript. C. Wend, C. Colonero, and E. Graham performed the DOC, stable isotope, and ICP-MS analyses, respectively. We thank all involved with coring operations. This research was supported by T. McCoy, Vice President for Research, Montana State University, and NSF grants OPP94-19413, OPP92-11773, OPP98-15512, and OPP98-15998.

Microorganisms in the Accreted Ice of Lake Vostok, Antarctica

D. M. Karl,[1] D. F. Bird,[2] K. Björkman,[1] T. Houlihan,[1] R. Shackelford,[1] L. Tupas[1]

Analysis of a portion of Vostok ice core number 5G, which is thought to contain frozen water derived from Lake Vostok, Antarctica (a body of liquid water located beneath about 4 kilometers of glacial ice), revealed between 2×10^2 and 3×10^2 bacterial cells per milliliter and low concentrations of potential growth nutrients. Lipopolysaccharide (a Gram-negative bacterial cell biomarker) was also detected at concentrations consistent with the cell enumeration data, which suggests a predominance of Gram-negative bacteria. At least a portion of the microbial assemblage was viable, as determined by the respiration of carbon-14–labeled acetate and glucose substrates during incubations at 3°C and 1 atmosphere. These accreted ice data suggest that Lake Vostok may contain viable microorganisms.

The existence of subglacial lakes in East Antarctica has been known for nearly three decades, but only recently have their large numbers and dimensions been revealed (1). Lake Vostok, one of nearly 80 subglacial lakes that have been discovered and mapped by means of airborne 60-MHz radio-echo sounding (2), is the largest (~14,000 km^2 surface area and ~1800 km^3 volume) and deepest (up to 670 m) of these unusual subglacial environments. The fresh water in Lake Vostok is kept liquid by the pressure of the ice overburden (equivalent to ~350 atm) and, perhaps, by geothermal heating. This lake and others like it may contain previously undescribed relic populations of microorganisms that are adapted for life in these presumably oligotrophic (low-nutrient, low-biomass, and low–energy flux) habitats.

In 1998, a team of Russian, U.S., and French scientists completed the drilling of Vostok hole number 5G (72°28′S, 106°48′E).

At a termination depth of 3623 m, this is the deepest ice core ever obtained. The bottom of the core is ~120 m from the ice–Lake Vostok water interface. The upper 3300 m of Vostok ice core 5G provides a continuous record of Earth's paleoclimate over the past 400,000 years, including four complete glacial-interglacial periods (3). Ice samples extracted from core depths of 1500 to 2750 m (with corresponding ages ranging from 110,000 to 240,000 years) have shown (i) the presence of a diverse assemblage of prokaryotic and eukaryotic microorganisms (0.8×10^3 to 11×10^3 cells per milliliter of ice melt), (ii) a positive correlation between the presence of dust and the number of microorganisms, and (iii) the presence of viable mesophilic microorganisms as revealed by the consumption of ^{14}C-labeled organic substrates (4).

At greater depths in Vostok ice core 5G, between 3311 and 3538 m, the layers are disturbed by ice sheet dynamics; and beneath 3538 m, changes in the crystal structure, electrical conductivity, and stable isotope and gas composition of the ice suggest that the basal ice at this location (3538 to 3743 m) is refrozen Lake Vostok water (3, 5). Because this lake is so remote and is largely inaccessible, the accreted ice provides the most reliable surrogate

sample of the Lake Vostok ecosystem before the actual penetration of the ice-lake boundary and the collection of water samples.

A sample of the accreted Lake Vostok ice was analyzed for (i) microbial cell enumeration by epifluorescence microscopy, scanning electron microscopy (SEM), and dual laser flow cytometry (Figs. 1 and 2); (ii) microbial biomass estimation with two independent biomarker compounds (Table 1): adenosine-5′-triphosphate (ATP) and lipopolysaccharide (LPS); (iii) microbial cell viability and potential metabolic activity by analysis of rates of ^{14}C-CO_2 production and ^{14}C-incorporation into macromolecules after timed incubations with exogenous ^{14}C-labeled organic substrates (Tables 1 and 2); and (iv) the presence of potential carbon and nitrogen growth substrates (6–9). Our measurements from ice collected at 3603 m complement the independent ice core analyses of a sample from 3590 m (10). A major difference is that our core contained no sediment inclusions. Therefore, the results presented here may not be directly comparable to those of Priscu et al. (10), despite the fact that both samples were obtained from the accreted ice of Lake Vostok.

Epifluorescence microscopic examination of decontaminated, melted ice samples revealed numerous inorganic particles, many of which fluoresced under ultraviolet (UV) illumination (Fig. 1). The presence of these particles complicates precise enumeration of putative microbial cells; however, microbial cells (presumably bacteria) were readily and unequivocally detected (Fig. 1, A and B). There was a spectrum of cell sizes and morphologies, ranging from the abundant small (0.1 to 0.4 µm) coccoid cells that represented about half (43 ± 6%) of the community to a diverse mixture of thin rods and vibrios (0.5 to 3 µm) that made up the remainder (Fig. 1). Enumeration revealed a relatively low abundance of 2×10^2 to 3×10^2 cells per milliliter of melted ice, which extrapolates to ~3 ng of C per liter (Table 1). These biomass estimates are at least an order of magnitude lower than estimates of total prokaryotic cells present in low-nutrient, deep ocean environments (Table 3).

[1]School of Ocean and Earth Science and Technology (SOEST), University of Hawaii, Honolulu, HI 96822, USA. [2]Département des Sciences Biologiques, Université du Quebec à Montreal, Casier Postal 8888, Succursale Centre-Ville, Montreal, QC, Canada, H3C 3P8.

Dual laser–based flow cytometric analyses of the ice melts confirmed the two main conclusions of the direct microscopic observations: (i) the presence of a broad size spectrum of particles with variable blue fluorescence, including DNA-containing microorganisms and (ii) the presence of fluorescent (especially red) inorganic particles (Fig. 2, A and B). Prokaryotic cell enumeration by the Hoechst 33342 staining method yielded estimates of 5×10^2 to 7×10^2 cells per milliliter of melt, a value that is about two to three times greater than the estimates based on microscopic observations. We believe that these higher estimates from the flow cytometric analyses are due to the inability of the method to discriminate between stained cells and stained nonliving particles of similar size (Fig. 2). In any case, even these estimates from flow cytometric analyses are low compared to biomass estimates from other oligotrophic aquatic ecosystems (Table 3).

Total LPS concentration was used as an independent estimate of the presence of bacterial cells. This cell wall biomarker is known to correlate with Gram-negative bacterial cell mass (11–13). From these LPS determinations, we estimate the Gram-negative bacterial biomass to be 0.5 to 1.6 ng of C per liter of ice melt (Table 1). This is about an order of magnitude lower than LPS concentrations reported from deep ocean environments (Table 3) and is consistent with the relatively low microbial biomass estimated from direct microscopy (Table 1). The lower LPS-extrapolated biomass, relative to direct microscopy and flow cytometry, might be expected if the microbial assemblages were not exclusively Gram-negative bacteria.

Attempts to measure ATP, an independent biomarker for microbial biomass (13, 14), were negative. This was in part due to the relatively high detection limit (≥ 0.5 pg of ATP ml^{-1} of melt, using a 50-ml sample) resulting from limitations in total sample volume. If total microbial biomass was ~1 to 3 ng of C per liter, as the direct count and LPS data suggest, then ATP in these samples would have been ~0.01 pg ml^{-1}, or undetectable by our protocols. Larger sample volumes, however, should provide an unequivocal quantification of viable cells by ATP detection.

Incubation of the ice melts with ^{14}C-labeled acetate and glucose documented the production of ^{14}C-CO$_2$, indicating the presence of metabolically active cells (Table 2). Acetate was respired 800 times more rapidly than was glucose (Tables 1 and 2). These respiration rates correspond to turnover times of approximately 2 and 2000 years, respectively, for the added organic substrates. Compared to ^{14}C-CO$_2$ production, rates of ^{14}C incorporation into macromolecules (such as nucleic acid and protein) were even lower (Table 2), if detectable at all. For ^{14}C-labeled acetate, the ^{14}C incorporated

into macromolecules (the sum of that incorporated into nucleic acid and protein) was only 0.1 to 0.2% of the ^{14}C respired; for ^{14}C-glucose, the relative incorporation was higher (10 to 40%), even though the total metabolism was lower (Table 1). Transfer of subsamples to 23°C after an initial 11-day incubation at 3°C stimulated ^{14}C-CO$_2$ production and ^{14}C-incorporation into macromolecules (Table 2). It should be emphasized, however, that these rates of organic matter mineralization are potential rates; in situ rates under ambient conditions (350 atm and subzero temperatures) may be much lower. Furthermore, the presence of liquid water would be required for cellular metabolism.

Inorganic and organic nutrient supply is the key to survival in all Earth habitats. The detection of relatively low total organic carbon (~7.5

Fig. 1. Microscopic analyses of melt samples from the accreted Vostok ice. (**A**) Epifluorescence. SYBR Green I–stained image of a small coccoid-shaped bacterium (right, bright yellow-green cell) and associated red-fluorescing non-living particulate matter. (**B**) Epifluorescence. SYBR Green I–stained image of a rod-shaped bacterium. (**C**) Field emission SEM image of a coccoid bacterium on a 0.02-μm Anopore filter viewed at a magnification of ×150,000 in the decontaminated ice melt. (**D**) SEM image of a rod-shaped bacterium as in (B).
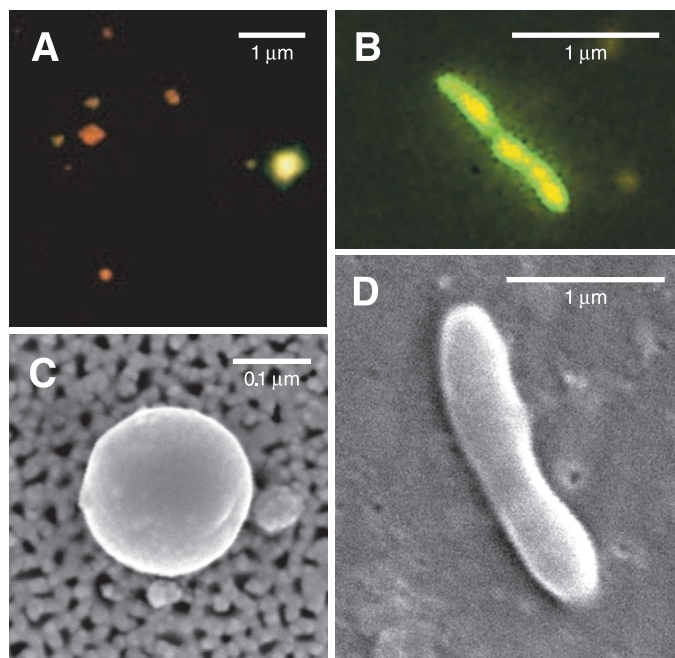

Fig. 2. Flow cytometric particulate matter analysis of a Hoechst 33342–stained top melt sample from the accreted Vostok ice. (**A**) A plot of log red fluorescence (relative units) versus log blue fluorescence (relative units) along with reference beads of known size and fluorescence intensity. Green indicates the population of particles with low blue (low DNA) and variable size [see (B)]; they were not counted as bacteria. (**B**) A plot of log blue fluorescence, same scale as in (A), versus log right angle side scatter (relative units) along with the same reference beads. We identified at least two particle categories: "heterotrophic bacteria" and high blue–high red–fluorescing particles. The heterotrophic bacteria designation is based on the known properties of marine bacteria with cell dimensions similar to those of the small coccoid-shaped bacteria in the ice core melts (Fig. 1). On the basis of these criteria, we estimate the bacterial abundances in the top melt and bottom melt samples to be 498 and 712 cells per milliliter, respectively. These values conform to those determined with direct microscopy and to cell carbon estimates derived from LPS concentrations (Tables 1 and 3).
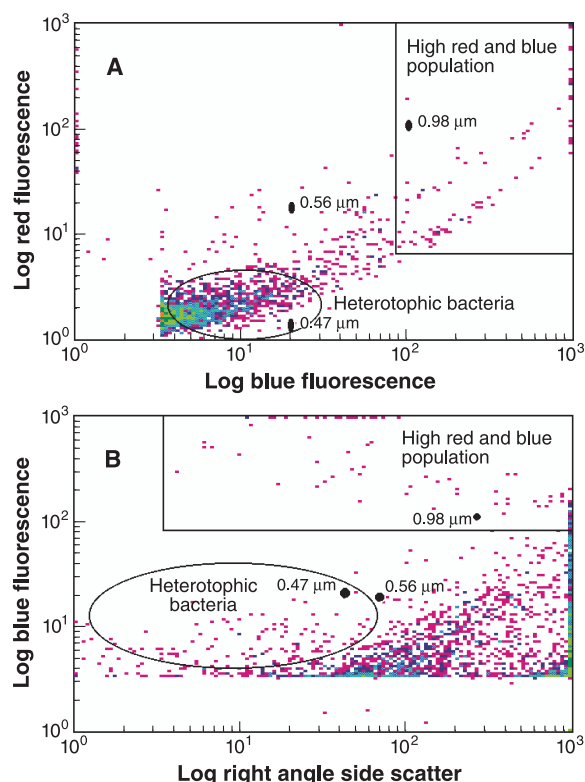
μM; Table 1) in the accreted ice, a value that is about five times lower than in deep ocean habitats (15), suggests that Lake Vostok is oligotrophic. In addition, we detected both oxidized and reduced nitrogen in the melt samples (Table 1). A reduction of nitrate plus nitrite in the accreted ice relative to concentrations in meteoric ice (16) might indicate net denitrification. The redox state of the lake is unknown, and some

geochemical models predict that most free oxygen might be sequestered in gas hydrates (17).

To survive in a liquid habitat for extended periods of time, microorganisms must have an exploitable energy source. If the energy for contemporary microbial populations in Lake Vostok is supplied from above, this lake may be one of the most oligotrophic habitats on Earth. Basal melting of the ice core and gravitational

transport would deliver deposited materials and ice-rafted debris, including microorganisms and potential growth substrates. If basin overflow connects these subglacial habitats to the sea (Lake Vostok is presently below sea level), this transport pathway could represent another allochthonous source of reduced carbon and energy. Alternatively, metabolic processes in the lake may be fueled by geothermal energy, analogous to microbial life discovered at deep sea hydrothermal vents (18). Lake Vostok may be associated with an intracontinental rift zone similar to that of East Africa, so this latter process remains a possibility (19). Finally, the subglacial lakes of East Antarctica may be among the most isolated ecosystems on Earth and could serve as terrestrial analogs to guide the design of samplers and experiments to be used in life probe missions to the ice-covered ocean of the jovian moon Europa (20).

Table 1. Selected chemical, biochemical, and microbiological measurements of decontaminated melt-water samples from the Vostok accreted ice at 3603 m.

Parameter*	Top melt	Bottom melt
$NO_3^- + NO_2^-$ (nmol liter^{-1})	170 ± 30	158 ± 28
TN (nmol liter^{-1})	972 ± 211	2577 ± 325
TOC (μmol liter^{-1})	7.5 ± 0.8	6.6 ± 2.9
ATP (ng liter^{-1})	<0.5	<0.5
LPS (ng liter^{-1})	0.095 ± 0.024	0.083 ± 0.021
Mean bacterial biomass (ng of C liter^{-1})†	0.6–1.6	0.5–1.4
Epifluorescence microscopy (cells ml^{-1})	291 ± 44	278 ± 43
Mean bacterial biomass (ng of C liter^{-1})‡	2.9 ± 0.4	2.8 ± 0.4
Respiration rate§		
Acetate (nmol of C liter^{-1} day^{-1})	434 ± 86	326 ± 168
Glucose (nmol of C liter^{-1} day^{-1})	0.53 ± 0.19	0.84 ± 0.72

*Values presented are mean estimates ±SD (n = 3 to 5). †Calculation assumes that all microorganisms are Gram-negative bacteria (they all contain LPS) and have a C:LPS ratio ranging from 6.7 to 16.7 (8). ‡Includes all prokaryotes that were not further separated by the methods used in the present study. Biomass extrapolation assumes 10 fg of carbon per prokaryotic cell. §Based on ^{14}C-CO_2 production measured with ^{14}C-labeled acetate and glucose during timed incubations at 3°C and 1 atm (8) (Table 2). Disintegrations per minute (DPM) per milliliter of sample per day were converted to nmol of C liter^{-1} day^{-1}, using uptake data and substrate-specific radioactivity and labeling information (8). The calculation of C flux for acetate assumes that carboxyl carbon tracks methyl carbon in metabolism, because only the methyl carbon was labeled with ^{14}C.

Table 2. Respiration and net incorporation of ^{14}C-labeled acetate and glucose by microorganisms in decontaminated meltwater samples from the Vostok accreted ice at 3603 m. ^{14}C activity is expressed as DPM of the specific ^{14}C-labeled organic substrate that was respired (CO_2) or incorporated into cellular biomolecules [nucleic acid (NA) and protein] per 2-ml sample of ice melt per incubation time, as indicated. All samples were corrected for time zero ^{14}C activities in the respective fractions: 190 (±16) DPM for $^{14}CO_2$ in glucose and 11,611 (±1556) DPM for $^{14}CO_2$ in acetate. No significant (above instrument background) amount of ^{14}C was detected in either the NA or protein fractions, so time zero procedural blanks were used for error propagation estimation: 25.9 (±1.9; n = 8) DPM of ^{14}C for NA and 25.8 (±3.8; n = 8) DPM of ^{14}C for protein. Values shown are mean net (experimental minus controls, or blanks) determinations ±1 SD (n = 3) for the 2- and 11-day incubations; all others are single net measurements. All incubations were conducted at 3°C in the dark, except as noted.*

Sample	Substrate	Incubation time (days)	^{14}C activity (DPM per sample)		
			CO_2	NA	Protein
Top melt	^{14}C-acetate	2	2,962 (±3,218)	−0.6 (±3.0)	2.2 (±5.5)
		11	24,388 (±9,054)	40 (±31)	0.9 (±1.8)
		18	36,560	6.9	27
		18 (23°C)*	113,045	983	2,258
	^{14}C-glucose	2	22 (±19)	2.1 (±3.1)	−2.1 (±4.9)
		11	77 (±19)	9.2 (±11.3)	−2.8 (±4.8)
		18	104	19	36
		18 (23°C)	17,893	599	764
Bottom melt	^{14}C-acetate	2	2,708 (±1,784)	0.2 (±3.2)	1.1 (±4.8)
		11	24,311 (±11,088)	59 (±17)	1.3 (±6.3)
		18	13,258	43	3.8
		18 (23°C)	166,341	1,528	4,007
	^{14}C-glucose	2	50 (±45)	3.2 (±2.7)	−2.7 (±5.5)
		11	67 (±21)	14 (±2.1)	−2.0 (±5.1)
		18	122	16	4.9
		18 (23°C)	42,741	956	1,674

*The data for the 18-day sample at 23°C were obtained by removing single replicate subsamples at the 11-day time point and incubating them for an additional 7 days at 23°C. A second replicate sample was kept at 3°C. The differences, therefore, between the treatments of the 18-day sample at 3°C and the 18-day sample at 23°C represent temperature-dependent changes in metabolism.

Table 3. Cross-ecosystem comparisons of microbial biomass for a variety of natural aquatic habitats. Habitat data are from a variety of sources (22). DMC, direct microscopic count.

Habitat	Depth (m)	Method	Estimated microbial biomass* (μg of C liter^{-1})
South Atlantic, off SW Africa	10	LPS	23
		DMC	14
	500	ATP	1.8
		LPS	1.6
		DMC	1.1
	1800	ATP	1.3
		LPS	0.7
		DMC	0.4
North Pacific, near Aleutian Trench	10	ATP	90–100
	1000	ATP	0.4
	4000	ATP	0.06
	7200	ATP	0.05
North Pacific gyre, near Hawaii	10	ATP	5–8
		LPS	2–4
		DMC	5
	1000	ATP	0.05–0.20
		LPS	0.04–0.06
	4500	ATP	0.01–0.04
		LPS	0.02–0.03
Galapagos Rift hydrothermal vent	2550	ATP	100–250
Subglacial Ross Sea, Antarctica (Station J-9)	237	ATP	0.01–0.13
		DMC	0.09–0.12
Dry Valley Lakes, Antarctica			
Lake Fryxell	5–18	DMC	5–436
Lake Hoare	5–30	DMC	3–668
Lake Bonney (East Lobe)	5–40	DMC	0.3–818
Vostak accreted ice	3603	ATP	<0.1
		LPS	0.001
		DMC	0.003

*Extrapolated using C:LPS = 11.7 (weight/weight), C:ATP = 250 (weight/weight), and 10 fg of C per bacterial cell.

References and Notes

1. G. K. A. Oswald and G. de Q. Robin, *Nature* **245**, 251 (1973); A. P. Kapitsa, J. K. Ridley, G. de Q. Robin, M. J. Siegert, I. A. Zotikov, *Nature* **381**, 684 (1996).
2. M. J. Siegert, J. A. Dowdeswell, M. R. Gorman, N. F. McIntyre, *Antarct. Sci.* **8**, 281 (1996).
3. J. R. Petit *et al.*, *Nature* **399**, 429 (1999).
4. S. S. Abyzov, I. N. Mitskevich, M. N. Poglazova, *Microbiology* **67**, 451 (1998).
5. J. R. Petit, in *Lake Vostok Workshop Final Report*, R. E. Bell and D. M. Karl, Eds. (National Science Foundation, Washington, DC, 1999), pp. 16–17; J. Jouzel *et al.*, *Science* **286**, 2138 (1999).
6. The ice core section analyzed in this study was obtained from the National Ice Core Laboratory. The sample, designated bag 3603, was a 50-cm-long (from 3602.5 to 3603.0 m) split of the 10-cm-diameter Vostok ice core, which was collected with the use of conventional electromechanical coring methods. Because these drilling procedures do not control for potential chemical and microbiological contamination, we devised a way to decontaminate the sample before analysis. First, the core was cut laterally into three approximately equal portions; two of these, designated "top" (465 g) and "bottom" (440 g), were immediately processed and a third portion was archived at −20°C. Our goal was to decontaminate the exterior surfaces of the ice core by a controlled melting process. The solvent used was commercially available, high-performance liquid chromatography water (HPLC-H₂O). After this rinsing procedure, the partially ablated decontaminated ice cores were placed in sterile plastic bags where they were allowed to completely melt at 0°C without added solvent. The rinse samples contained both the solvent (HPLC-H₂O) and partially melted ice proportions that were determined gravimetrically. The final melts were considered to be uncontaminated, undiluted, Vostok accreted ice and were the focus of this study. The decontamination of the top section of the ice core removed 248 g (53% by weight) into 1017 g of HPLC-H₂O (final concentration, 20% ice). This procedure yielded two separate ice samples: top rinse I and top melt. The bottom portion of the core was decontaminated in a two-step rinse procedure. In the first treatment, 108 g of ice (25% by weight) was melted in 505 g of HPLC-H₂O (final concentration, 18% ice), and in the second rinse 66 g of ice (15% by weight of the original ice sample) was melted into 518 g of HPLC-H₂O (final concentration, 11% ice). This procedure yielded three separate ice samples: bottom rinse I, bottom rinse II, and bottom melt. Visual inspection of the partially ablated ice cores before final melting revealed an apparently homogeneous solid with no evidence of fissures, cracks, or other imperfections.
7. Particle analysis and bacterial cell enumeration were done as follows. Subsamples (1 ml each) for epifluorescence microscopy, SEM, and flow cytometry were preserved with 20% 0.02 μm–filtered paraformaldehyde (final concentration, 1%) and immediately frozen in liquid nitrogen. The samples were stored at −80°C until analyzed. Samples of 1 ml were prepared for epifluorescence microscopic enumeration by filtration onto an Anopore filter (16 mm in diameter; pore size, 0.02 μm), followed by staining with SYBR Green I [R. T. Noble and J. A. Fuhrman, *Aquat. Microbiol. Ecol.* **14**, 113 (1998)] and mounting in 60% glycerin–phosphate-buffered saline containing vitamin A (5 mg ml⁻¹) and vitamin E acetate (2 U ml⁻¹). Bacteria were identifiable as bright yellow-green cells. Epifluorescence counts were made by four complete transects across the filter at ×1000 magnification; standard errors of the mean count averaged 14%. Photographs were taken with Kodak Ektachrome 400 ASA slide film. Samples (1 ml) were also prepared for SEM by filtration onto a small area of either a prewashed polycarbonate filter (pore size, 0.05 μm) or a 0.02-μm Anopore filter, which was dehydrated with ethanol, dried with liquid carbon dioxide at the critical point, and then coated with gold. The samples were examined with a Hitachi field emission SEM, model S-4700. In the SEM, bacteria were identified by their electron density and their shape, as well as by their elemental composition by energy dispersive analysis of x-rays. Photographs were taken at ×20,000 to ×150,000 magnification with a resolution of 2048 ×

2048 pixels. Images were sharpened by unsharp-masking in Adobe Photoshop 4.0. Finally, subsamples (1 ml) were analyzed by colinear dual-beam flow cytometry with a Coulter EPICS 735 instrument (*21*). Hoechst 33342, a DNA-specific dye, was used to stain microbial cells. A 225-mW UV light laser aligned colinear with a 1-W visible (488 nm) laser permitted simultaneous estimation of forward angle light scatter, right angle light scatter (RALS), blue (DNA) fluorescence (BF), and red autofluorescence for single particles that were passed through the detection port by means of a microsample delivery system. Bacteria were identified as a distinct cluster on a scatter plot of BF versus RALS (*21*). A known concentration of size-sorted beads was used as an external calibration. Bacterial cell number was extrapolated to cell carbon content by assuming a per cell carbon quota of 10 fg [J. R. Christian and D. M. Karl, *J. Geophys. Res.* **99**, 14269 (1994); R. Fukuda, H. Ogawa, T. Nagata, I. Koike, *Appl. Environ. Microbiol.* **64**, 3352 (1998)]. For ATP analysis, subsamples (50 ml) were acidified with H₂SO₄ (final concentration, 0.1 M) and stored at 4°C until processed. ATP standards were prepared at the same time, using HPLC-H₂O as the solvent. MgCl₂ (final concentration, 10 mM) and NaOH (final concentration, 10 mM) were added to effect the formation of Mg(OH)₂, which quantitatively coprecipitates ATP. The isolated Mg(OH)₂-ATP was dissolved in HCl, and the ATP was measured with the firefly bioluminescence reaction (K. Björkman and D. M. Karl, in preparation). The detection limit of the procedure used was 0.5 pg of ATP per milliliter of the sample (10⁻¹² M). Total LPS (dissolved plus particulate) concentrations were measured in undiluted samples with the use of the turbidimetric *Limulus* amoebocyte lysate (LAL) assay [S. W. Watson, T. J. Novitsky, H. L. Quinby, F. W. Valois, *Appl. Environ. Microbiol.* **33**, 940 (1977)] (*12*) and a computer-assisted commercially available instrument (LAL-5000; Associates of Cape Cod). Gram-negative bacterial cell carbon was estimated by assuming that LPS ranged from 6 to 15%, by weight, of total cell carbon, which corresponds to a C:LPS conversion factor of 6.7 to 16.7 (*11*). The detection limit for this assay was 0.025 pg of LPS per milliliter, and internal endotoxin standard recovery was 42.3 ± 5.1%.
8. For analysis of metabolic activity, two 18-ml aliquots of each sample were transferred to clean, sterile polypropylene tubes and spiked with 5 μCi of either [2,¹⁴C]-acetate (catalog number NEC-085, NEN Life Sciences; specific activity, 2 mCi mmol⁻¹) or D-[¹⁴C(U)]-glucose (catalog number NEC-042, NEN Life Sciences; specific activity, 3.4 mCi mmol⁻¹). These substrate additions were equivalent to 139 and 82 μM for acetate and glucose, respectively. The samples were mixed, then dispensed (2 ml each) into a series of eight sterile, 30-ml, glass serum bottles, which were fitted with a gas-tight red rubber stopper containing a plastic center well with a fluted filter paper (Whatman no. 2) wick [J. E. Hobbie and C. C. Crawford, *Limnol. Oceanogr.* **14**, 528 (1969)]. The samples were placed into a 3°C incubator in the dark. A set of time zero control samples was also prepared and processed. After 2- and 11-day incubation periods at 3°C, triplicate subsamples were removed and processed for ¹⁴C-CO₂ and ¹⁴C-incorporation into nucleic acid and protein. At the 11-day sampling point, one of the remaining two subsamples for each treatment was removed from the 3°C incubator and was placed at 23°C for an additional 7-day period. The last subsample was kept at 3°C. These final samples (18 days at 3°C and 18 days at 23°C) were also processed for ¹⁴C-CO₂, ¹⁴C–nucleic acid, and ¹⁴C-protein. First the fluted filter paper was wetted with 100 μl of the CO₂-trapping solvent β-phenylethylamine, using a gas-tight syringe. Next, without removing the serum stoppers, 2 ml of H₂SO₄ (2 M) was injected directly into the sample. This acidification step terminated the incubation, precipitated cellular macromolecules, and forced any ¹⁴C-CO₂ that was present into the head space. The samples were placed at room temperature for a 24-hour passive distillation of ¹⁴C-CO₂ into the β-phenylethylamine–soaked filter paper contained in the center well. The stoppers were then removed, and the wicks were placed into liquid scintillation vials containing 10 ml of Aquasol-II as the fluor and counted for ¹⁴C activity. The acidified samples were transferred into

clean test tubes and processed for ¹⁴C incorporation into nucleic acid and protein fractions [D. M. Karl, *Appl. Environ. Microbiol.* **44**, 891 (1982)].
9. Potential growth substrates were analyzed as follows. Nitrate plus nitrite (NO₃⁻ + NO₂⁻), total nitrogen (TN), and total organic carbon (TOC) concentrations were measured in the decontaminated top and bottom melts. For (NO₃⁻ + NO₂⁻), melt water was acidified and chemically reduced to produce a quantitative yield of nitric oxide (NO), which was measured with a commercially available nitrogen oxidizer [C. Garside, *Mar. Chem.* **11**, 159 (1982)]. The detection limit for this high-sensitivity chemiluminescence method was 10 pmol of N, using a 10-ml sample (1 nM). Internal standards added to samples of the accreted ice were recovered quantitatively. TN was measured by high-temperature (1110°C) combustion and chemiluminescence detection using nitrate as the standard [T. W. Walsh, *Mar. Chem.* **26**, 295 (1989)]. Before analysis, the top and bottom ice melts were concentrated 10-fold using a Speedvac evaporator system. The TN method measures all particulate and dissolved pools. Reduced N (ammonium plus organic N) is calculated by difference ([TN] − [NO₃⁻ + NO₂⁻]). TOC was measured by means of a high-temperature (800°C) combustion oxidation method [J. Qian and K. Mopper, *Anal. Chem.* **68**, 3090 (1996)] with an automated TOC analyzer (MQ Scientific model 1001). Potassium hydrogen pthalate was used as the standard. Certified reference materials were used to establish instrument blank (0 μM DOC sample) and to determine measurement accuracy. Internal standards were recovered quantitatively.
10. J. C. Priscu *et al.*, *Science* **286**, 2141 (1999).
11. M. Maeda and N. Taga, *J. Appl. Bact.* **47**, 175 (1979).
12. S. W. Watson and J. E. Hobbie, in *Native Aquatic Bacteria: Enumeration, Activity and Ecology*, J. W. Costerton and R. R. Colwell, Eds. (American Society for Testing and Materials, Philadelphia, PA, 1979), pp. 82–88.
13. D. M. Karl and F. C. Dobbs, in *Molecular Approaches to the Study of the Ocean*, K. E. Cooksey, Ed. (Chapman & Hall, London, 1998), pp. 29–89.
14. D. M. Karl, *Microbiol. Rev.* **44**, 739 (1980).
15. J. H. Sharp *et al.*, *Mar. Chem.* **48**, 91 (1995).
16. M. Legrand and P. Mayewski, *Rev. Geophys.* **35**, 219 (1997).
17. M. C. Kennicutt II, T. Sowers, B. Lyons, J. R. Petit, in *Lake Vostok Workshop Final Report*, R. E. Bell and D. M. Karl, Eds. (National Science Foundation, Washington, DC, 1999), pp. 26–28.
18. H. W. Jannasch and C. O. Wirsen, *BioScience* **29**, 592 (1979); D. M. Karl, in *The Microbiology of Deep-Sea Hydrothermal Vents*, D. M. Karl, Ed. (CRC Press, Boca Raton, FL, 1995), pp. 35–124.
19. I. Dalziel, in *Lake Vostok Workshop Final Report*, R. E. Bell and D. M. Karl, Eds. (National Science Foundation, Washington, DC, 1999), pp. 17–19.
20. S. W. Squyres, R. T. Reynolds, P. M. Cassen, S. J. Peale, *Nature* **301**, 225 (1983); M. H. Carr *et al.*, *Nature* **391**, 363 (1998); C. R. Chapman, *Science* **283**, 338 (1999); T. B. McCord *et al.*, *Science* **280**, 1242 (1998).
21. B. C. Monger and M. R. Landry, *Appl. Environ. Microbiol.* **59**, 905 (1993).
22. Habitat data were taken from the following sources. South Atlantic: (*12*). Aleutian Trench: O. Holm-Hansen, R. Hodson, F. Azam, in *Analytical Applications of Bioluminescence and Chemiluminescence*, E. W. Chappelle and G. I. Picciolo, Eds. (NASA SP-388, Washington, DC, 1975), pp. 75–87. North Pacific gyre: (*13*); R. P. Shackelford, thesis, University of Hawaii (1998); the Hawaii Ocean Time series online database (http://hahana.soest.hawaii.edu/hot/hot_jgofs.html). Galapagos Rift: D. M. Karl, C. O. Wirsen, H. W. Jannasch, *Science* **207**, 1345 (1980). Subglacial Ross Sea: F. Azam *et al.*, *Science* **203**, 451 (1979). Antarctic Dry Valley lakes: C. D. Takacs and J. C. Priscu, *Microb. Ecol.* **36**, 239 (1998).
23. We thank R. Bell and J. Priscu for invaluable discussions of Lake Vostok; K. Selph for the flow cytometric analyses; H. Vali, H. Campbell, and M. Lagacé for electron microscopy; B. Bays for preparation of Fig. 1; and L. Lum for assistance in the preparation of this manuscript. Supported by NSF (grant number OPP96-32763). This is SOEST publication 4931.